

Structural anomaly in superconductivity of CaFe_2As_2 class of materials

Ram Prakash Pandeya¹, Arindam Pramanik¹, Anup Pradhan Sakhya¹, Rajib Mondal¹, A. K. Yadav², S. N. Jha², A. Thamizhavel¹ and Kalobaran Maiti^{1*}

¹ *Department of Condensed Matter Physics and Materials Science, Tata Institute of Fundamental Research, Homi Bhabha Road, Colaba, Mumbai - 400 005, INDIA.*

² *Nuclear Physics Division, Applied Spectroscopy Division, Bhabha Atomic Research Centre, Mumbai - 400 085, INDIA.*

(Dated: December 22, 2024)

Quantum transitions in Fe-based systems are believed to involve spin, charge and nematic fluctuations. Complex structural phase diagram in these materials often emphasizes importance of covalency in their exotic properties, which is directly linked to the local structural network and barely understood. In order to address this outstanding issue, we investigate the evolution of structural parameters and their implication in unconventional superconductivity of 122 class of materials employing extended x -ray absorption fine structure studies. The spectral functions near the Fe K - and As K -absorption edge of CaFe_2As_2 and its superconducting composition, $\text{CaFe}_{1.9}\text{Co}_{0.1}\text{As}_2$ ($T_c = 12$ K) exhibit evidence of enhancement of Fe contribution with Co-substitution near the Fermi level. As-Fe and Fe-Fe bondlengths derived from the experimental data exhibit interesting changes with temperature across the magneto-structural transition. Curiously, the evolution in Co-doped composition is similar to its parent compound despite absence of magneto-structural transition. In addition, we discover anomalous change of Ca-X ($X = \text{Fe}, \text{As}$) bondlengths with temperature in the vicinity of magneto-structural transition and disorder appears to be less important presumably due to screening by the charge reservoir layer. These results reveal evidence of doping induced evolution to the proximity to critical behavior presumably leading to superconductivity in the system.

PACS numbers: 61.05.cj, 74.70.Xa, 75.30.Fv

While high temperature superconductivity continues to be an outstanding puzzle in contemporary condensed matter physics, the Fe-based systems revealed additional complexity in the problem. It appears that complex interplay of spin, orbital, charge and lattice degrees of freedom is responsible for the exoticity of these materials [1]. Parent compound of almost all the Fe-based materials exhibit a structural transition from tetragonal phase possessing C_4 symmetry to an orthorhombic phase, where the 4-fold rotational symmetry is broken leading to nematicity in the system [1, 2]. Some studies pointed out importance of charge reservoir layer in the electronic properties [3, 4]. Electronic properties of these systems have been studied extensively using angle-resolved photoemission spectroscopy (ARPES), scanning tunnelling spectroscopy, etc. [5–9]. However, the structural aspects remains to be still illusive, in particular, the role of local structural parameters in the electronic properties.

In order to address this issue, we employed extended x -ray absorption fine structure (EXAFS) studies to probe the evolution of structural parameters of a archetypical compound CaFe_2As_2 (Ca122), a parent Fe-based superconductor in the 122 class of material and its Co-doped composition, $\text{CaFe}_{1.9}\text{Co}_{0.1}\text{As}_2$ (CaCo122), which shows superconductivity below 12 K. Ca122 has been studied extensively and shows both structural and magnetic transition from tetragonal paramagnetic phase to orthorhombic-antiferromagnetic phase below 170 K [10]. In addition, it exhibits complex phase diagram as a function of pressure; application of a small pressure (~ 0.35

GPa) helps to retain its tetragonal symmetry, which is called a collapsed tetragonal (cT) phase [11–15]. The cT phase can be obtained by other means too such as chemical substitution at any of three atomic sites and/or quenching from a temperature higher than 700 °C to room temperature [16]. Even the ambient pressure phase shows signature of cT phase in its electronic structure [17]. Many studies showed superconductivity on application of pressure and/or doping [15, 18–22], while some other studies did not find superconductivity in the cT phase [23]. Evidently, superconductivity in this system is complex along with additional complexity arising due to structural and magnetic interactions. Exploiting EXAFS, we found intriguing results in Ca122 and CaCo122 systems revealing an interesting structural link to superconductivity of this material.

Single crystalline samples were grown using Sn flux [24, 25] and characterized by powder x -ray diffraction and energy dispersive analysis of x -rays measurements. Magnetic susceptibility measurements [10] exhibit sharp antiferromagnetic transition at 170 K in Ca122. A sharp diamagnetic transition below 12 K is observed in CaCo122 indicating its superconducting phase in the ground state. Temperature dependent EXAFS measurements were carried out in transmission mode at BL-8 beamline at INDUS-2, RRCAT, Indore, India [26].

In Fig. 1(a), we show Fe K -edge and Co K -edge x -ray absorption spectra of CaCo122 collected at 300 K. The near edge regimes are shown in expanded energy scales in Fig. 1(b) and Fig. 1(c) exhibiting similar features indi-

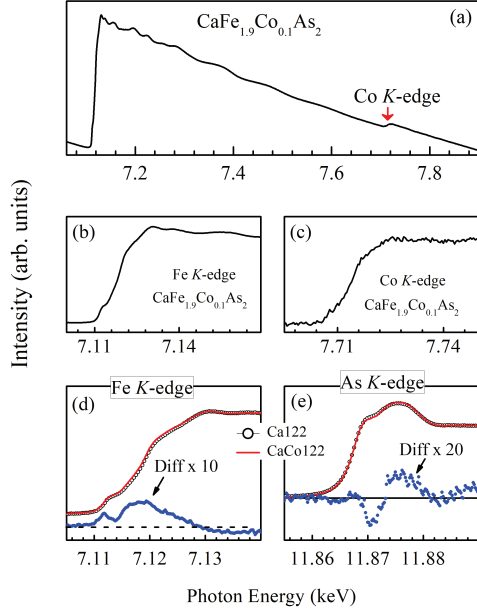


FIG. 1. (a) Fe K -edge absorption spectrum of CaCo122 collected at 300 K. Co K -edge is shown by an arrow. Expanded view of (b) Fe K -edge and (c) Co K -edge regimes. Comparison of the (d) Fe K -edge and (e) As K -edge data taken from Ca122 (open circles) and CaCo122 (line). Rescaled difference spectra (CaCo122 data - Ca122 data) are shown at the bottom panel (solid circles).

cating similarities in the transition metal $4p/3d$ contributions in the unoccupied part of the electronic structure. This also demonstrates extended nature of the electronic states that smeared out disorder due to chemical substitution. The Fe K -edge and As K -edge spectra of Ca122 and CaCo122 are shown in Fig. 1(d) and Fig. 1(e), respectively. Fe K -edge data reflect the unoccupied part of the Fe $4p$ partial density of states (PDOS), which also contains Fe $3d$ PDOS due to finite pd hybridization. On the other hand, As K -edge data reflect the unoccupied As $4p$ states consisting of symmetry adapted Fe $3d$ contributions due to strong Fe $3d$ -As $4p$ covalency. The energies of the experimental spectral features appear very close to those found in the EXAFS database for Fe and As elemental metals. This suggests that the effective charge states of Fe and As in these compounds are close to their elemental metallic state as also observed in other Fe-based systems [27]. Electronic configuration close to neutral Fe and As atoms in Ca122 has also been observed in high resolution hard x -ray photoelectron spectroscopic studies [14].

We have superimposed the Ca122 and CaCo122 data in Fig. 1(d) and Fig. 1(e) to investigate the changes due to Co substitution. While the raw data look close to each other, the difference spectra (see solid circles in the lower

panel of the figure) exhibit interesting features. The difference spectrum at Fe K -edge exhibits an enhancement in intensity with two distinct peaks; a narrower one at the edge and a broader one at higher energy. Co-substitution at the Fe-sites leads to doping of electrons. Therefore, the change at the absorption edge is expected as follows: (i) a shift of Fermi level to higher energy, which will increase the binding energy of the core levels defined with respect to the Fermi level and/or (ii) change in charge states of both the atoms of quasi-2D FeAs layers. In contrast, the feature at the edge in Fig. 1(d) exhibits shift of the Fermi level towards lower energies. The As K -edge data exhibits a depletion of intensity at the edge; weaker intensity compared to that at the Fe K -edge could be due to weaker contribution of As $4p$ states near Fermi level [4]. Clearly, the hybridization of As $4p$ states with Fe $3d$ gets modified with an effective spectral weight transfer to higher energies. One possible reason of shift of the edge in Fe K -edge data to lower energy could be due to stronger pd hybridization leading to an enhancement of Fe $4p$ population and thereby pulls the $4p$ contributions towards lower energies. Clearly, Fe PDOS enhances at the Fermi level with the Co-substitution.

The Fourier transform (FT) of the k^2 -weighted EXAFS oscillations were calculated using a Hanning window of $3 - 15 \text{ \AA}^{-1}$ in the k -axis; due to the presence of Co K -edge at Fe K -edge spectra of CaCo122, the window kept within 12 \AA^{-1} . We have verified in Ca122 case that this change in k -range does not have significant effect on the results. FTs corresponding to the Fe K -edge and As K -edge data of Ca122 are shown in Fig. 2(a) and Fig. 2(b) for Fe K -edge and As K -edge data and the same for CaCo122 sample are shown in Fig. 2(c) and Fig. 2(d), respectively; black to orange lines correspond to the spectrum collected at 300 K to 12 K temperatures. We observe significant decrease in intensity and interesting change in the peak position of the features with the increase in temperature. While the peak position remain almost unchanged at the As K -edge data even if the temperature is increased from 12 K to 300 K, the peak at Fe K -edge exhibit different scenario. The most intense peak at the Fe K -edge of Ca122 sample shifts towards lower values with the increase in temperature indicating compression in contrast to the expected expansion. In addition, Fe K -edge data of CaCo122 sample exhibit distinct two peak structure (A and B in the figure) between 2-3 \AA ; the relative intensity of B with respect to that of A reduces significantly with the increase in temperature.

To extract the parameters related to the local structure, the radial distribution of FT amplitudes shown in Fig. 2, were modeled by the conventional approach based on single scattering approximation. The crystal structure and atomic positions in Ca122 are well studied employing high resolution x -ray and neutron diffraction [10–12], which is used as a guide for the analysis of the EXAFS oscillation. As atoms are surrounded by a tetrahedral

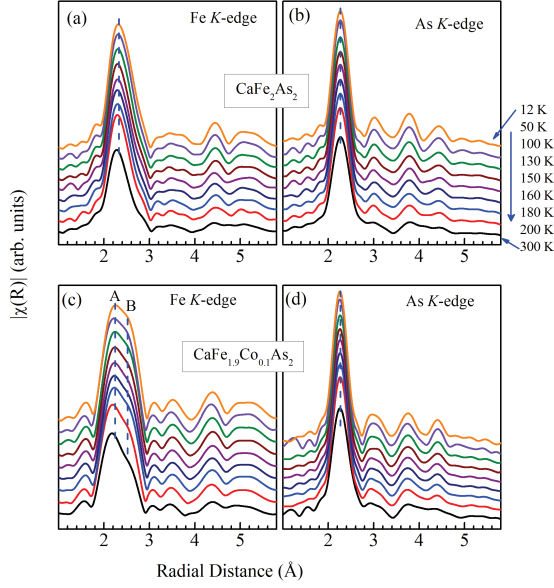


FIG. 2. Fourier transform of the temperature dependent k^2 weighted EXAFS oscillations extracted from (a) Fe K -edge and (b) As K -edge data of Ca122. Similar results for CaCo122 at (c) Fe K -edge and (d) As K -edge.

cage formed by four Fe atoms and FeAs bond length is 2.4 Å. Fe-Fe distances form the next neighbour separations within the Fe layer. Since the distortion due to structural transition is small, we report the results corresponding to effective tetragonal structure for clarity in presentation. The initial parameters for different bonds were calculated using the structural parameters obtained from neutron diffraction technique [11]. The Fe-As and Fe-Fe distances are very close to each other. Thus, the first shell of Fourier transform obtained from Fe K -edge EXAFS oscillations is contributed by both Fe-As and Fe-Fe bonds as evident in the Fig. 2(a) and 2(c). However, the first shell of As K -edge data possesses contribution only from the As-Fe bonds [28, 29]. Therefore, the local structure information related to the Fe-As bonds is extracted from As K -edge, which is used to extract the information about Fe-Fe bonds from FT of Fe K -edge EXAFS oscillations first shell [29].

Extracted bondlengths are shown in Fig. 3 exhibiting intriguing temperature dependence. The results for the parent compound, Ca122 shown by open circles exhibit significant change in bond distances across the magnetic and structural phase transition temperature of 170 K. The As-Fe bondlength gradually decreases from the room temperature across the magneto-structural transition and eventually stabilizes at lower temperatures. Instead, the Fe-Fe distance increases gradually and saturates below the transition temperature. These results re-

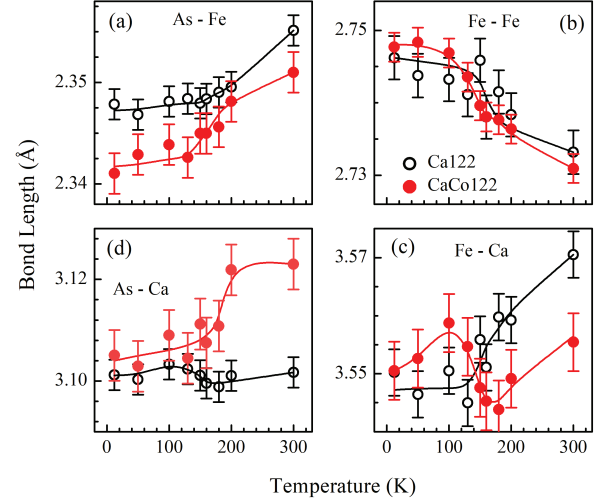


FIG. 3. (a) As-Fe, (b) Fe-Fe, (c) As-Ca and (d) Fe-Ca bondlengths as a function of temperature in Ca122 (open circles) and CaCo122 (solid circles). Solid lines are the smooth curves drawn as a guide to the eye. Bond distances with Ca exhibit interesting temperature evolution.

veal decrease in anion height with the decrease in temperature and hence, stronger Fe-As hybridization along with a decrease in Fe-Fe direct overlap within the xy -plane. Ca layers exhibit an unusual scenario; while the As-Ca distance marginally increases across the phase transition, Fe-Ca distance reduces significantly with the decrease in temperature indicating stronger overlap of Ca $4s$ states with the Fe $3d$ states indicating important role of Ca-sites as found in other systems [30]. The thermalization of the bondlengths appears to occur at temperature (~ 100 K), which is much below the transition temperature.

In CaCo122, the As-Fe distance becomes smaller than that in the parent compound. Although no magnetic transition is observed in this material, we observe a significant dip spreading over a wider temperature range at the low temperature side. Fe-Fe distance also exhibit similar behavior. As-Ca distance is larger in the doped sample than the distance in the pristine one. Below 200 K, the As-Ca distance exhibit a stiff decrease and becomes close to the values in the pristine sample below 100 K. Fe-Ca distance exhibit anomalous evolution - at room temperature, the bondlength is smaller in the doped sample and gradually reduces with the temperature as expected. Below 200 K, it exhibits sudden jump to a higher value and again starts reducing below 100 K. Clearly, onset of magnetic interactions at low temperature induces significant structural reorganization and a new structural order seems sets in below 100 K. The structural transition in Ca122 leads to a reduction of rotational symmetry from

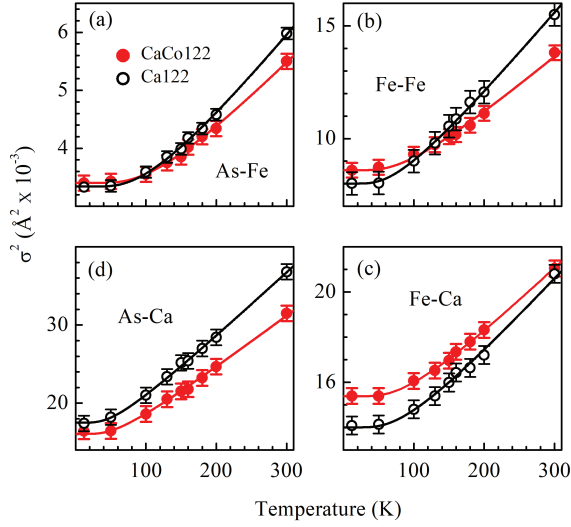


FIG. 4. Debye-Waller factor corresponding to (a) As-Fe, (b) Fe-Fe, (c) Fe-Ca and (d) As-Ca bonds in Ca122 (open circles) and CaCo122 (solid circles). Lines are the fit employing Einstein model.

C4 (tetragonal) to C2 (orthorhombic) phase which is defined as nematicity. Recent studies revealed signature of hidden C4 phase (collapsed tetragonal phase) even in the parent compound at ambient pressure probably due to strain [17]. Evidently, Co-substitution in Ca122 brings the system closer to its magneto-structural transition leading to an enhanced nematic fluctuations and absence of magnetic order although magnetic interactions are present as in Ca122 indicating its proximity to quantum criticality. Moreover, Ca appears to play an important role in deriving the electronic properties.

We estimated the Debye-Waller factor (DWF), σ^2 associated to each pair of atoms; the results (symbols) are shown in Fig. 4. In every case, DWF gradually reduces with the decrease in temperature and gets saturated at very low temperatures. This typical behavior is in line with the expected behavior arising from thermal contributions. We do not observe any anomaly across the structural and magnetic phase transition temperature indicating little influence of disorder on the phase transitions in this material while other systems show different behavior [31]. The DWF for As-Fe is found to be the smallest compared to all other cases. The values for As-Fe and Fe-Fe bonds are quite similar in both the pristine and doped compound. However, DWF for As-Ca bond is smaller in the doped sample and that for Fe-Ca bond becomes higher in the doped sample. In contrast to the expected enhancement of disorder due to chemical substitution, the disorder in this system reduces with Co-substitution except the Fe-Ca case, which is longest bond among the

TABLE I. Local structure parameters obtained from temperature dependent of Fe and As K -edge EXAFS measurements on CaFe_2As_2 ($\text{CaFe}_{1.9}\text{Co}_{0.1}\text{As}_2$).

Bonds	Θ_E (K)	ω_E (meV)	k ($\text{eV} \cdot \text{\AA}^{-2}$)	σ_o^2 (\AA^2)
Fe-As	310 (337)	25.8 (28.0)	5.1 (6.0)	0.001 (0.001)
Fe-Fe	224 (256)	18.6 (21.3)	2.3 (3.0)	0.003 (0.004)
Fe-Ca	244 (251)	20.3 (20.9)	2.3 (2.4)	0.010 (0.011)
As-Ca	150(167)	12.5 (13.9)	1.0 (1.2)	0.011 (0.011)

cases discussed here.

Using Einstein model of crystal vibration [32], DWF is given by, $\sigma^2 = \sigma_o^2 + (\hbar/2\mu\omega_E)\coth[(\hbar\omega_E)/(2k_B T)]$, where μ , ω_E and σ_o^2 are the reduced mass, the Einstein frequency and temperature independent DWF, respectively. For a given pair of atoms of mass m_1 and m_2 , the reduced mass, $\mu (= m_1 m_2 / (m_1 + m_2))$ is independent of temperature and σ_o^2 is linked to the lattice disorder. The temperature dependent part is related to the thermodynamic properties of the material and allows us to derive the Einstein temperature, $\Theta_E (= \hbar\omega_E/k_B)$ and the effective spring constant, $k_{eff} (= \mu\omega_E^2/2)$. The lines passing through the symbols in the Fig. 4 represent the least square error fits and provide an excellent representation of the experimental results within the Einstein model.

The extracted parameters for Ca122 and CaCo122 are given in the Table. I. In Ca122, the Einstein temperature, Θ_E is 310 K (215 cm^{-1}) for Fe-As bond, which is very close to the measured Raman shift in Ca122 for E_g mode (211 cm^{-1}); Fe and As atoms oscillate opposite to each other in respective ab planes [33]. The Einstein temperature for Fe-Fe is smaller than that for Fe-Ca suggesting weaker Fe-Fe direct overlap relative to Fe-Ca bonding. It is smallest for As-Ca bond (150 K). The Einstein frequency and spring constant is the largest for Fe-As bond; these results once again establish strong covalency between Fe $3d$ - As $4p$ states. Bonding with Ca seems to be weaker but significant along with a larger static disorder, σ_o^2 .

With Co-substitution, the Einstein temperature, Einstein frequency and spring constant enhances significantly keeping the static disorder close to the values in parent compound. The enhancement of the parameters for Fe-Fe bonds is somewhat larger than the other cases. It appears that the dominance of the spring constant, Einstein frequency, etc associated to the Fe-sites play major role in the superconducting composition. This has also been manifested in the near-edge data, where we observed enhancement of intensity and a shift of the absorption edge to lower energies due to Co-substitution.

The large σ_o^2 value obtained for both As-Ca and Fe-Ca bonds are quite high indicating large disorder at Ca sites. Recent angle-resolved photoemission study [17] revealed signature of collapsed tetragonal phase hidden even within the ambient band structure, which corre-

spond to a slightly smaller lattice constant, c . Thus, one reason for higher σ_0^2 could be this hidden structure. In any case, presence of larger disorder associated to Ca-site maintaining other cases small indicate that the disorder arising due to chemical substitutions are essentially absorbed by the Ca-layer as expected for a charge-reservoir layer in such materials.

In summary, we have studied the role of structural parameters in the electronic properties of Ca122 with an emphasis on their evolution in achieving superconductivity. Fe contribution near Fermi level appear to be larger in superconducting composition relative to the parent compound. In CaFe_2As_2 , the bondlengths gradually changes over a wide temperature range; the change in parameters starts at a temperature much higher than the magneto-structural transition temperature of 170 K providing evidence of a precursor effect [34, 35]. A flattening of the bondlengths occurs below 100 K indicating achieving the structural parameters close to its ground state configuration. Curiously, similar behavior is observed in the Co-doped sample too which is superconducting and does not show magneto-structural transition. Disorder appear to be similar in both the cases despite the chemical substitution in the superconducting material. Interestingly, the bond-length involving Ca sites in the superconducting composition exhibit anomalous behavior in the vicinity of magneto-structural transition. While these results reveal complex structural link and importance of charge reservoir layer in superconductivity, we discover evidence of the survival of electronic interactions of the parent compound in the superconducting composition - a key feature of critical behavior.

Authors acknowledge RRCAT, Indore for their support in carrying out experiments and financial support under the project no. 12-R&D-TFR-5.10-0100. KM acknowledges financial assistance from DST, Govt. of India under J. C. Bose Fellowship program and DAE under the DAE-SRC-OI Award program.

* Corresponding author: kbmaiti@tifr.res.in

[1] H. Hosono *et al.*, Sci. Technol. Adv. Mater. **16**, 033503 (2015).

- [2] G. R. Stewart, Rev. Mod. Phys. **83**, 1589 (2011).
- [3] T. H. Geballe and G. Koster, What Tc Can Teach About Superconductivity, pages 325-344, Handbook of High Temperature Superconductivity, Springer New York, (2007).
- [4] K. Ali and K. Maiti, Sci. Rep. **7**, 6298 (2017); *ibid.* The Eur. Phys. J. B **91**, 199 (2018).
- [5] S. Tan *et al.*, Nat. Mater. **12**, 634-640 (2013).
- [6] C. Liu *et al.*, Phys. Rev. Lett. **101**, 177005 (2008).
- [7] A. Charnukha *et al.*, Sci. Rep. **5**, 10392 (2015).
- [8] G. Adhikary *et al.*, J. Phys.: Condens. Matter **25**, 225701 (2013).
- [9] J. E. Hoffman, Rep. Prog. Phys. **74**, 124513 (2011).
- [10] N. Ni *et al.*, Phys. Rev. B **78**, 014523 (2008).
- [11] A. Kreyssig *et al.*, Phys. Rev. B **78**, 184517 (2008).
- [12] A. I. Goldman *et al.*, Phys. Rev. B **78**, 100506(R) (2008).
- [13] D. K. Pratt *et al.*, Phys. Rev. B **79**, 060510(R) (2009).
- [14] R. P. Pandeya *et al.*, J. Phys: Condens. Matter (Letter) DOI: <https://doi.org/10.1088/1361-648X/ab86ff>.
- [15] M. S. Torikachvili, Sergey L. Budko, Ni Ni, and Paul C. Canfield, Phys. Rev. Lett. **101**, 057006 (2008).
- [16] R. S. Dhaka *et al.*, Phys. Rev. B **89**, 020511 (R) (2014).
- [17] K. Ali *et al.*, Phys. Rev. B **97**, 054505 (2018); G. Adhikary *et al.*, J. Appl. Phys. **115**, 123901 (2014); K. Maiti, Pramana - J. Phys. **84**, 947 (2015).
- [18] Y. Qi *et al.*, EPL **96**, 47005 (2011).
- [19] S. R. Saha *et al.*, Phys. Rev. B **85**, 024525 (2012).
- [20] K. Kudo *et al.*, Sci. Rep. **3**, 1478, (2013).
- [21] D-Y Chen *et al.*, Chin Phys. Lett. **33**, 6 067402 (2016).
- [22] Kui Zhao *et al.*, PNAS, **113**, 46 12969 (2016).
- [23] W. Yu *et al.*, Phys. Rev. B **79**, 020511(R) (2009).
- [24] N. Kumar *et al.*, Phys. Rev. B **79**, 012504 (2009).
- [25] R. Mittal *et al.*, Phys. Rev. Lett., **102**, 217001 (2009).
- [26] D. Joseph, A. K. Yadav, S. N. Jha, and D. Bhat-tacharyya, Bull. Mater. Sci., **36**, 1067 (2013).
- [27] E. m. Bittar *et al.*, Phys. Rev. Lett. **107**, 267402 (2011).
- [28] B. Joseph *et al.*, Phys. Rev. B **82**, 020502 (2010).
- [29] M. Y. Hacısalıhıoglu *et al.*, Phys. Chem. Chem. Phys., **18**, 9029 (2016).
- [30] D. Lahiri *et al.*, Phys. Rev. B **82**, 094440 (2010); R. S. Singh and K. Maiti, Phys. Rev. B **76**, 085102 (2007).
- [31] R. Bindu, K. Maiti, S. Khalid, and E. V. Sampathkumar, Phys. Rev. B **79**, 094103 (2009); R. Bindu, K. Maiti, R. Rawat, and S. Khalid, Appl. Phys. Lett. **92**, 121906 (2008).
- [32] E. Sevilano, H. Meuth and J. J. Rehr, Phys. Rev. B **20**, 4908 (1979).
- [33] K.-Y. Choi *et al.*, Phys. Rev. B **78**, 212503 (2008).
- [34] K. Maiti *et al.*, Phys. Rev. Lett. **95**, 016404 (2005).
- [35] P. L. Paulose, N. Mohapatra, and E. V. Sampathkumar, Phys. Rev. B **77**, 172403 (2008).